J Comp Physiol A (1986) 158:625–637

Journal of Comparative Physiology A Sensory, Neural, and Behavioral Physiology

In vivo visualization of individual neurons in arthropod ganglia facilitates intracellular neuropil recording

Heinrich Reichert and Wulf Dieter Krenz
Department of Zoology, University of Basel, Rheinsprung 9, CH-4051 Basel, Switzerland

Accepted February 17, 1986

Summary. A simple method for the in vivo visualization of dye filled cells by laser illumination is used to characterize neurons in situ in the segmental ganglia of the locust and the crayfish (Fig. 1). Neuron visualization provides the structural information necessary for identification of cells during an ongoing physiological experiment (Figs. 2, 3). Sequential penetrations of soma and neuropil as well as simultaneous double neuropil penetrations of spiking and nonspiking cells are facilitated by the visual control afforded by neuron visualization (Figs. 4, 5, 6). Furthermore, neuron visualization allows the sampling of cellular properties at multiple, predetermined sites in the dendritic and axonal arbors of identified neurons (Fig. 7) and aids in establishing synaptic connectivity through double neuropil recordings (Fig. 8).

Introduction

The physiological analysis of individual neurons in arthropod nervous systems has profited greatly from intracellular staining techniques (Stretton and Kravitz 1968; Pitman et al. 1972; Stewart 1978). It has become routine to stain an intracellularly penetrated cell by injection of dye from the recording electrode following its physiological characterization. Structure and neurophysiological properties are then often adequate to identify uniquely the so characterized cell (see Hoyle 1977).

Usually, however, the structure of a dye-filled neuron is determined after removal of the ganglion from the animal, followed by histological processing (e.g. Kater and Nicholson 1973; Strausfeld and Miller 1980). Thus structural information is not available *during* the physiological experiment. This restrains the experimental protocol considerably. For example, it is often not possible to identify an impaled cell during the experiment. Precise localization of the site of penetration as well as multiple penetrations of a given cell are difficult. Moreover, finding cells that are postsynaptic to the impaled neuron is difficult, since the location of the neuron's axonal arborizations is usually not known. These difficulties are compounded whenever it becomes necessary to obtain intracellular recordings from the neuropil of arthropod neurons, as often occurs when one wants to study synaptic potentials or their subthreshold interactions. Such recordings must be established and maintained 'blind', i.e., without being able to see the target neurons. In sum, many of the difficulties involved in recording from arthropod neurons are related to the lack of visual control over the impaled neurons during the physiological experiment.

In this report we describe a simple method for the in vivo and in situ visualization of dye-filled neurons in segmental ganglia of the locust and the crayfish. This procedure, an adaptation of a technique developed by Miller and Selverston (1979) and modified by Jacobs and Miller (1985), involves injection of Lucifer yellow into neurons and subsequent visualization of the cells with a low intensity blue light laser. We show here that this method can be used to overcome many of the problems involved in carrying out single and multiple neuropil penetrations of arthropod neurons.

Materials and methods

Animals. Experiments were carried out on crayfish (*Procambarus clarkii* or *Astacus leptodactylus*) or on locusts (*Locusta migratoria*) obtained from commercial suppliers. Crayfish were kept in running-water aquaria at 12 °C on a 12 h/12 h light-dark

cycle. Locusts were kept in crowded laboratory cultures at 30 °C on a 17 h/7 h light-dark cycle.

Preparations. Experiments were performed on sensory interneurons in the crayfish terminal ganglion and on flight interneurons and motoneurons in the thoracic ganglia of the locust.

Experiments on crayfish were carried out using the isolated tailfan preparation described by Sigvardt et al. (1982). The abdominal central nervous system was isolated from an animal together with the tailfan, which was left attached to the abdominal CNS by the terminal ganglion peripheral nerves. This preparation was pinned down ventral side up in a Sylgard® lined dish and covered with crayfish saline. The terminal ganglion was desheathed for easier intracellular penetration of neurons. In some experiments water displacements were generated by a sinusoidally oscillating cylindrical probe which moved through the saline-air interface.

Experiments on locusts were carried out using the preparation described by Robertson and Pearson (1982). Locusts were pinned down on a wax block dorsal side up. A longitudinal incision was made through the thoracic tergites. The thoracic ganglia were then exposed by removing overlying gut and musculature. The meso- and metathoracic ganglia were stabilized for intracellular recordings on a metal spoon and covered with locust saline. All flight muscles except the dorsolongitudinal muscles were denervated. Flight motor activity was induced by blowing wind on the head of the animal and monitored by electromyogram recordings from the dorsolongitudinal flight muscles.

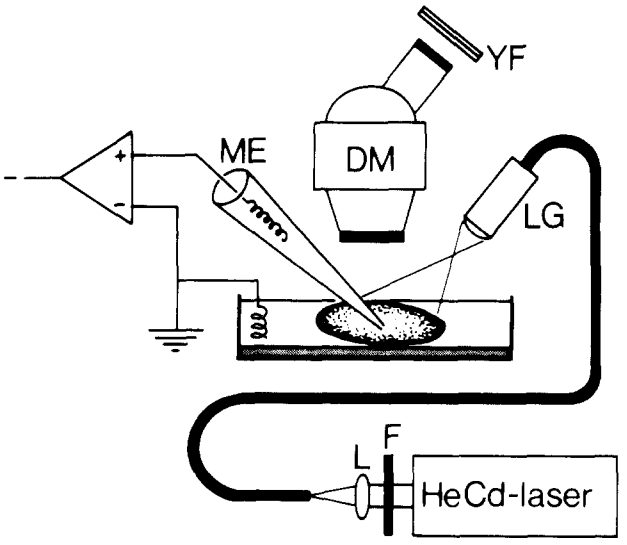

Fig. 1. Schematic illustration of the laser illuminator

Intracellular recording and staining. Intracellular recordings were carried out using microelectrodes made from 1 mm OD thick-walled (locust neurons) or thin-walled (crayfish neurons) micropipettes (Hilgenberg) on a Brown and Flaming electrode puller (Sutter Instruments). The tips of the microelectrodes were backfilled with an 8% solution of Lucifer yellow in water; the electrode shanks were filled with a 1 molar Li^+-acetate solution. Electrode resistances were typically 40–100 MΩ. A Getting Model 5 intracellular preamplifier was used for recording and current injection. Physiological recordings were displayed conventionally and stored on an FM tape recorder (Racal). A signal averager (Tracor Northern) could be used on- or off-line.

Neurons were stained during the physiological experiment by injection of Lucifer yellow dye into the cell from the recording electrode. In neuropil penetrations, low intensity (1–3 nA), long duration (20–60 min) DC hyperpolarising current was usually used to fill neurons with dye. (Using greater amounts of hyperpolarizing current often resulted in relatively high intracellular concentrations of Lucifer yellow. Cells filled this way were more susceptible to damage from laser irradiation.) For filling cells from their soma, higher hyperpolarizing currents of up to 10 nA were used.

Laser illuminator and illumination procedure. For in vivo and in situ visualization, dye-filled neurons were illuminated by blue light emitted from a 40 mW He-Cd laser (Omnichrome Laser, Newport Corporation, Fountain Valley, California). The laser was fitted with an electromagnetic shutter and a neutral density filter holder for gross light intensity control. The coherent light beam was focused onto the end of a 3 m long armor cabled fiber light guide connected between a laser coupling head on one end and a handpiece on the other (Model F-LFI Laser-Fiber Illuminator, Newport Corporation). The laser beam was coupled into the fiber through an AR coated lens in the coupling head. Fine position adjustments centered the focused beam onto the fiber end. The optics in the handpiece on the output end of the fiber focused the emerging light beam to a spot diameter of approximately 0.5 mm at a focal distance of 5 cm. The maximal intensity of illumination of the focus of this lens was 1.4 mW cm^{-2}. Figure 1 shows a schematic illustration of the laser illuminator.

For cell illumination the emitting end of the light guide was hand held and directed towards the ganglion which contained the impaled and dye-filled cell. The preparation was viewed through a stereo dissecting microscope (Wild M5). The oculars of the microscope were fitted with yellow cutoff filters (Cokin, France), which blocked reflected blue light while allowing the yellow fluorescence of dye-filled illuminated cells to pass. Optimal intensity of illumination was attained simply by moving the light guide relative to the preparation under visual control.

For the visualization of dye-filled cells, both the intensity and the duration of illumination were kept as low as possible, since prolonged or intense illumination of Lucifer yellow filled cells resulted in toxic effects (see also Miller and Selverston 1979). The following procedures were found to be helpful in attaining adequate cell visualization with minimal illumination. (i) Visualization experiments were carried out after dark adaptation of the experimenter. (ii) For penetrations under visual control, cells were not visualized constantly during the electrode positioning process. Rather, cells were visualized briefly (less than 1 s) and a penetration site selected. This site was then related to a ganglion landmark, such as a neighboring cell body or a tracheal branch. Initial microelectrode positioning was carried out relative to this landmark. The cell was then visualized again briefly for fine positioning of the microelectrode tip. The strong fluorescence of the dye filled microelectrode aided in exact positioning of the electrode tip and did not interfere with seeing the cell. (iii) During and after illumination of impaled neurons, their resting membrane potential and input resistance were frequently monitored. An experiment was terminated if a cell which had been illuminated showed any changes in these two parameters. Other physiological properties of the neurons such as spike shape, synaptic potentials or burst type were also

monitored at regular intervals and used as indicators of cell viability whenever possible.

Cell anatomy. At the end of an experiment the structure of dye-filled neurons was documented either by photography of the cells in situ or by conventional whole mount histology or by both. For in situ photography a Wild Photomakroskop was used. The objective of the Photomakroskop was fitted with a yellow cutoff filter. The cell was illuminated with laser generated blue light and photographed in the living preparation. The short depth of field of the optics used for in situ photography made it somewhat difficult to photographically reproduce the entire three dimensional structure of the dye-filled neurons. For whole mount histology, the ganglia containing dye-filled cells were removed from the preparation and fixed for several hours in 10% buffered paraformaldehyde. They were then dehydrated in an alcohol series, cleared in methyl salicylate and viewed by epifluorescence microscopy. Stained cells were photographed and their structure drawn with a drawing tube.

Results

Identification of impaled neurons by in situ visualization of structure

In favorable cases an impaled neuron can be identified in situ and in vivo on the basis of its structure alone. Figure 2 shows such a neuron in the mesothoracic ganglion of the locust. The cell can be identified in situ (Fig. 2A) by the location of its soma, the characteristic branching pattern of its major dendrites and the nerve in which its axon leaves the ganglion as flight motoneuron no. 85, the pleuroaxillary (Pflüger et al. 1985). Figure 2B shows the structure of this neuron as seen with a compound fluorescence microscope after histological processing. Figure 2C shows intracellular recordings from the cell. Both confirm the in vivo identification of flight motoneuron no. 85. Note that the structure of the cell as seen after conventional histological processing is more detailed than that seen using the in vivo visualization technique. This is especially true for the fine branching pattern of the neuropil processes and for the precise location of the neuron's cell body. However, the salient features of the cell, those which are necessary for neuron identification, can be determined from the in vivo visualization of the neuron alone. Note also that both the dendritic arbors, which lie near the dorsal surface of the ganglion and the cell body, which is located on the ventral surface of the ganglion can be readily visualized.

Generally, both physiological properties of an intracellularly penetrated neuron and information about the cell's structure are necessary for neuron identification. With in situ visualization, both can be determined during the ongoing intracellular experiment. Figure 3 shows the results of an intracellular recording from a second flight motoneuron in the locust. The physiological recordings from this cell indicate that it is a wing elevator motoneuron (Fig. 3A). The structure of the cell as determined in vivo by laser visualization after injection of Lucifer yellow (Fig. 3B) together with this physiological data identifies the cell as wing elevator no. 113, the tergosternal. This is because the tergosternal is the only wing elevator in the metathoracic ganglion which (i) has an axon exiting the ganglion through the 3rd root and (ii) extends its neuropilar branches to the ganglion midline (Hedwig and Pearson 1984). Figure 3C shows the struc-

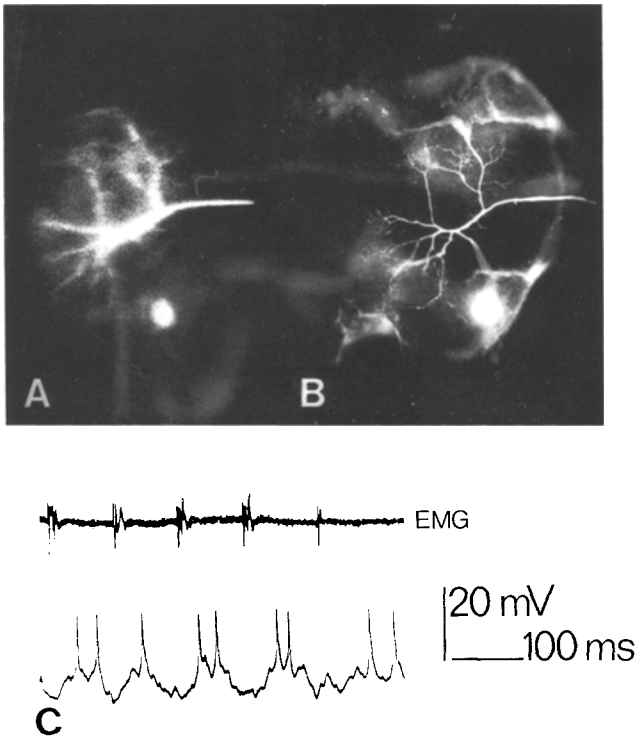

Fig. 2A–C. In vivo visualization of cell structure completely identifies a motoneuron in the locust. **A** Photomicrograph of a neuron visualized in vivo and in situ. The neuron was penetrated and filled with dye in the mesothoracic ganglion of the locust. Its structure as visualized in vivo by laser illumination reveals a ventral cell body, an axon which exits the ganglion through nerve root 3 and a characteristic branching pattern of the main dendritic arbors. These structural features identify this cell as flight motoneuron 85. (In this and all subsequent photomicrographs the recording microelectrodes were removed from the neurons prior to photography.) **B** Photomicrograph of the same cell after histological processing as seen through a fluorescence compound microscope. The structure of the cell is more detailed than that seen using the in vivo visualization technique. This is due to the histological clearing process, which reduces light diffusing properties of the fixed ganglion and also eliminates light reflection on the ganglion surface. **C** An intracellular recording from this motoneuron during the expression of flight motor activity together with an electromyogram from the dorsolongitudinal depressor muscle (*EMG*)

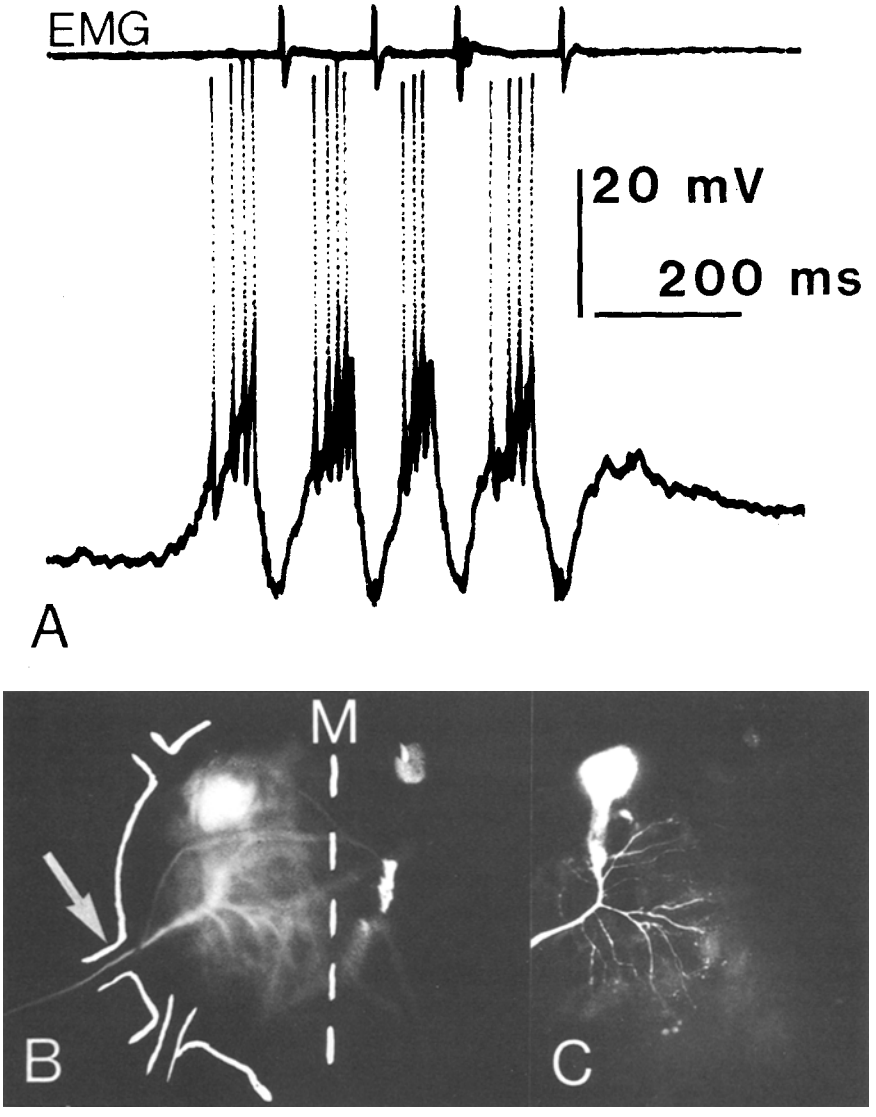

Fig. 3A–C. Intracellular physiology and in vivo visualization of structure identify a motoneuron in the locust. **A** Intracellular recording from a neuron in the metathoracic ganglion of the locust together with an electromyogram from the dorsolongitudinal depressor muscle (*EMG*) during flight motor activity. The neuron is active in antiphase to the depressor muscle. **B** Photomicrograph of the cell's structure as visualized in vivo. Note that the cell's axon exits the ganglion through the 3rd root (arrow) and that neuropil processes extend to the ganglion midline (dashed line). These anatomical features together with the physiological characterization of the neuron as elevator-phase identify the cell as flight motoneuron 113. **C** Photomicrograph of the same cell after histological processing

ture of the same neuron as determined after histological processing.

Sequential penetration of soma and neuropil in the same neuron

Recordings from the neuropil of arthropod neurons are generally more informative than those made from cell bodies. However, neuropil recordings have several technical disadvantages compared with cell body recordings. One is that they are harder to establish than soma recordings because the neuropil of (unstained) cells is invisible, whereas the somata of most cells are visible in unstained ganglia. Once established, neuropil recordings are harder to maintain. The neuropil processes are usually smaller than the soma of a neuron, thus a penetration in the neuropil is easier to lose. Repenetration of a cell in the neuropil is difficult for the same reasons. These disadvantages can be overcome by penetrating the soma, injecting the cell with dye, and then impaling the cell in the neuropil under visual control.

Figure 4A shows an example of this procedure applied to an interneuron in the crayfish terminal ganglion. The cell was first penetrated in the soma. It was then briefly visualized by laser illumination and a second microelectrode positioned above a desired neuropil recording site under visual control. In the first electrode passage, the neuropil of the interneuron was penetrated. Thus, not only was the neuropil penetration established rapidly, the site of intracellular penetration was also known – and specifically selected – prior to the physiological characterization of the cell. The signal decrement which is seen in soma recordings as com-

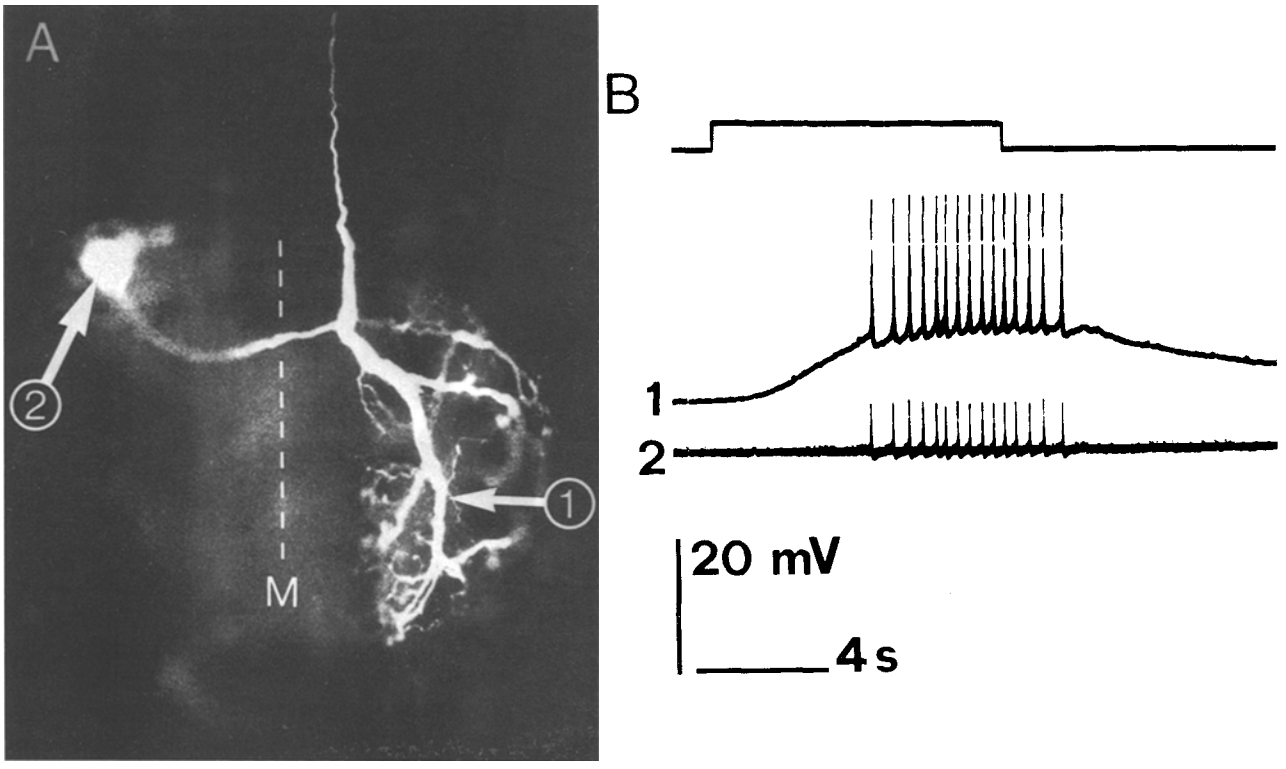

Fig. 4A, B. A neuropil recording is established under visual control following penetration and staining of the neuron's soma. **A** Photomicrograph of a crayfish sensory interneuron as seen after histological processing. This interneuron, the caudal photoreceptor, was penetrated with a dye filled electrode in its cell body (site '2') and filled with dye from there. Subsequently, the interneuron was visualized in vivo and penetrated with a second microelectrode in one of its main neuropil arbors (site '1'). M indicates the ganglion midline. **B** Intracellular recordings from neuropil and soma at sites '1' and '2' during presentation of a light pulse. Top trace, light monitor, middle trace, neuropil recording; bottom trace, soma recording (AC-coupled)

pared to neuropil recordings is clearly revealed in the simultaneous double intracellular penetration (Fig. 4B).

We have also repeatedly carried out the opposite procedure. A cell was first penetrated and characterized in the neuropil and filled with dye from there. Then the soma of the cell was visualized and penetrated with a second microelectrode. This type of experimental protocol is useful when stability problems arise, which make it hard to maintain a neuropil penetration in a given cell over a long time span. Such problems occur regularly when one attempts to penetrate two synaptically interconnected neurons within the same ganglion.

Double neuropil penetrations of single neurons

A further technical disadvantage of neuropil recordings is that their precise interpretation depends on knowledge of the site of penetration in the neuron. Electrical potentials recorded in the soma are usually attenuated, but for a given cell, they are attenuated in a reproducible way from preparation to preparation. A neuropil recording, on the other hand, will produce quantitatively different physiological data depending on the location of the site of penetration relative to the sites of origin of synaptic potentials or impulse initiation. In such cases, visualization of the electrode penetration site in a dye filled cell as described above can be useful. One can relate intracellular recordings to defined parts of the neuropil of a visualized cell and so obtain information on dendritic electroanatomy and on the location of synaptic inputs or their effects on spike generation. Moreover, one can obtain this type of information more readily by establishing *simultaneous* double neuropil recordings in the same neuron at precisely determined penetration sites.

Figure 5A shows a depressor flight motoneuron in the locust for which a simultaneous double neuropil recording was carried out. The cell was first penetrated at the site indicated by electrode '1'. It was then filled with dye and penetrated under visual control with a second microelectrode at the site indicated by electrode '2'. In the follow-

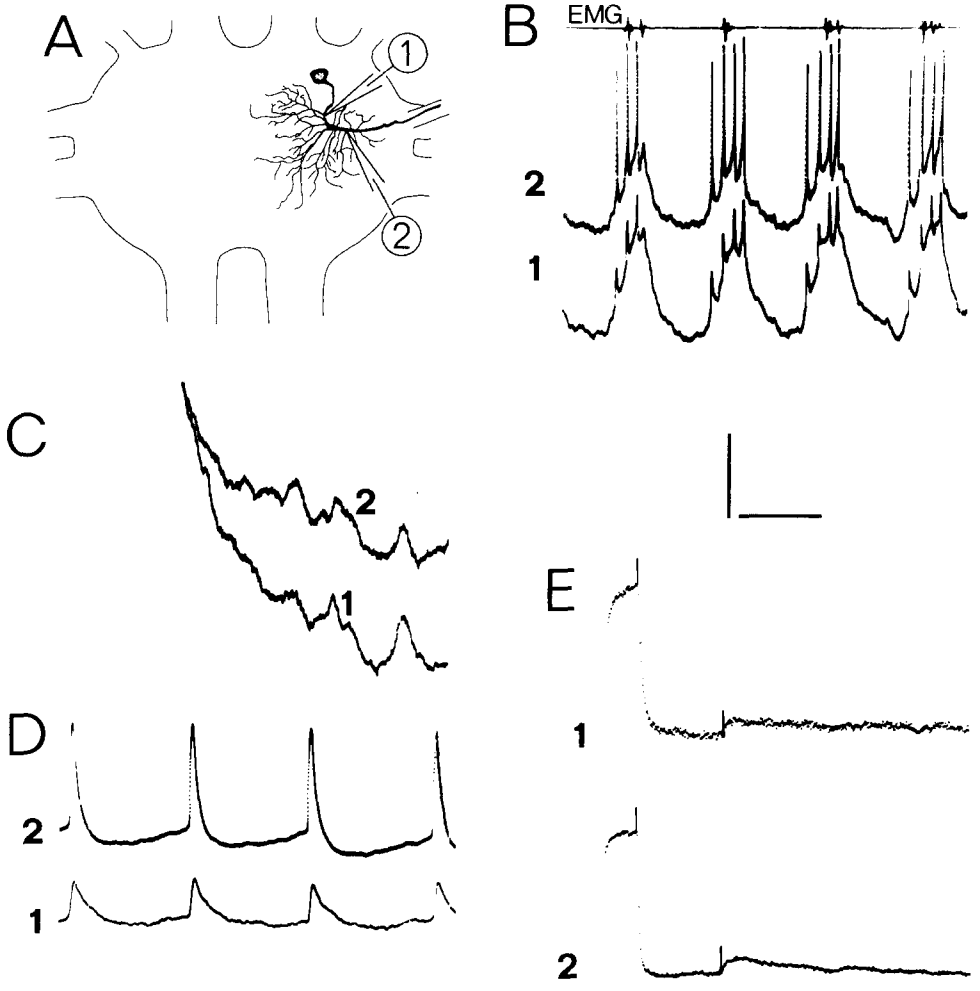

Fig. 5A–E. Simultaneous double neuropil recordings from a locust flight motoneuron. **A** Drawing of the structure of a flight motoneuron as seen after histological processing. This flight motoneuron was penetrated and filled with dye in its neuropil at site '1'. It was then visualized and penetrated with a second microelectrode at site '2'. **B** Intracellular recordings from the two neuropil sites '1' and '2' together with an electromyogram from the dorsolongitudinal depressor muscle (EMG) during flight motor activity. The motoneuron is a depressor and is identified on structural and physiological criteria as flight motoneuron 127. **C** Expansion of one portion of the flight motor activity shown in B at higher gain. Note that some of the PSPs visible in this part of the recording are larger at recording site '2' whereas others are larger at recording site '1'. **D** Intracellular recordings from the two neuropil sites during a spontaneous burst of action potentials in the motoneuron. Spikes are larger at site '2' indicating that this site is closer to the impulse initiation zone than site '1'. **E** Signal averaged recordings (24×) of the direct EPSP produced in the motoneuron by stimulation of the left ocellus with a light-off stimulus as recorded at the two neuropil sites (see Reichert and Rowell 1984, for stimulus specifications). The light-off stimulus occurs at the end of the 5 mV, 10 ms calibration pulse. Amplitude and time course of the signal averaged EPSP recorded at sites '2' and '1' are similar. Latency to onset of the EPSP is 22.8 ms at both sites. Scale bars: **B** 20 mV, 20 mV, 100 ms; **C** 5 mV, 5 mV, 20 ms; **D** 20 mV, 20 mV, 20 ms; **E** 3 mV, 3 mV, 23 ms

ing physiological characterization of the cell we asked two questions concerning the location of synaptic inputs.

First, flight motoneurons of this type receive rhythmically modulated drive from the elements of the flight pattern generator. Does this drive impinge onto spatially restricted parts of the motoneuron's neuropil or is it more distributed in nature? Figure 5B shows the response of the motoneuron recorded by the two microelectrodes during the expression of flight motor activity. An expansion of one portion of the activity in Fig. 5B is shown in Fig. 5C. Inspection of the relative amplitudes of PSPs derived from the pattern generator, as recorded at the two sites, shows that some of these PSPs are larger at the recording site '1', while others are larger at recording site '2'. This suggests that flight pattern generator input to the motoneuron is in fact distributed and is not convergently focussed onto one specific dendritic arbor.

Second, these motoneurons receive sensory input from numerous exteroceptive and proprioceptive sensory structures. Intracellular neuropil recordings indicate that some of this input, such as that derived 'directly' from the animal's ocelli (Rowell and Pearson 1983), is small and may not contribute significantly to motoneuron firing. Is this the case or are such recordings biased by the location of the recording electrode? A comparison of spike amplitudes in Fig. 5D indicates that electrode '2' is closer to the site of impulse initiation than electrode '1'. Figure 5E shows the size of a 'direct' ocellar mediated EPSP at the two recording sites. Note that the signal averaged values of the EPSP recorded at the two sites are comparable. Thus this type of ocellar mediated EPSP appears to be similarly small in magnitude irrespective of where in the major neuropil branches it is recorded. Accordingly, its effect on impulse initiation in flight motoneurons is judged to be small (Reichert and Rowell 1985).

Double simultaneous penetrations of the same cell are particularly important in studying the cellular properties of local, nonspiking interneurons. For example, neurons of this type may have input and output sites which are spread diffusely throughout their dendritic arbors or they may be polarized into special input and output domains (see Roberts and Bush 1981). This can be determined by penetrating the neuron with two microelectrodes, each placed in different defined parts of the cell, and then studying the amplitude and time course of the synaptic potentials recorded by the two electrodes.

Figure 6 shows an identified nonspiking local interneuron in the crayfish for which this was carried out. This cell, the LDS interneuron (Reichert et al. 1983), receives EPSPs from afferents which run in the peripheral nerves ipsilateral to the cell's soma. These EPSPs can cause postsynaptic inhibition of projecting sensory interneurons on the opposite, contralateral side of the cell. The cell also receives depolarizing IPSPs from afferents which run in the peripheral nerves contralateral to its soma. We wanted to know on which side of the LDS interneuron the EPSPs and the IPSPs originate. To determine this, a simultaneous double neuropil penetration was established at the recording sites indicated in Fig. 6A. Afferent roots ipsilateral to the cell's soma were stimulated electrically. The EPSPs resulting from this stimulation had a faster rise time, and higher peak amplitude in the neuropil ipsilateral to the cell's soma (Fig. 6B). In contrast, when afferent roots on the contralateral side were electrically stimulated

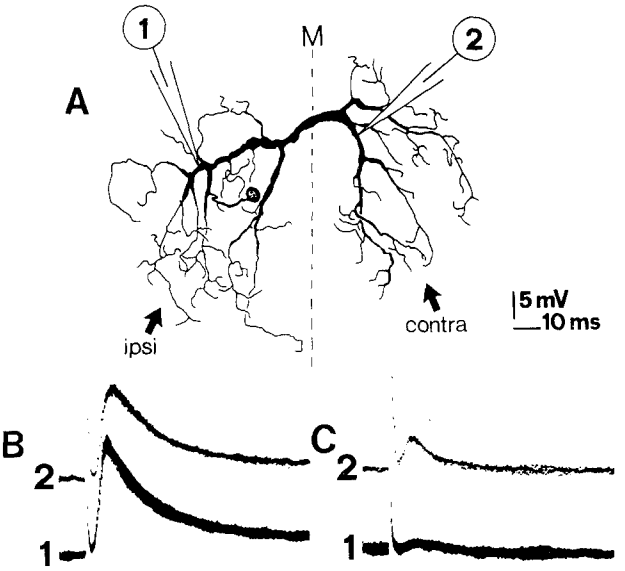

Fig. 6A–C. Simultaneous double neuropil recording from a nonspiking local interneuron in the crayfish (from Krenz and Reichert 1985). **A** Drawing of the structure of the interneuron as seen after histological processing. This interneuron, an LDS cell, was penetrated and filled with dye at site '1'. Thereafter it was visualized and penetrated with a second microelectrode at site '2'. The response of the cell to electrical stimulation of nerve roots ipsilateral and contralateral to the cell's soma was then determined. **B** The compound EPSP recorded at sites '1' and '2' in response to stimulation of the ipsilateral 3rd root. The EPSP has a shorter latency to onset, a faster rise time and a larger amplitude at site '1' than at site '2'. **C** The compound depolarizing IPSP recorded at sites '1' and '2' in response to stimulation of the contralateral 3rd root. The IPSP has a shorter latency to onset, a faster rise time and a larger amplitude at site '2' than at site '1'. Note that the decrement of the IPSP as recorded between the two penetration sites is about 70%, whereas the decrement of the EPSP is only about 15%. This may be due to a decrease in membrane resistance caused by the shunting inhibitory action of the IPSP

(Fig. 6C), the resulting depolarizing IPSPs had a faster rise time and higher peak amplitude in the contralateral neuropil. These results indicate that the ipsilateral soma side of the cell is the main input side for the EPSPs and that the contralateral side is the main input side for the IPSPs (Krenz and Reichert 1985).

Sampling physiological properties sequentially at multiple sites in one neuron

As mentioned above, simultaneous penetrations of different neuropil arbors can provide information on the way in which signals are generated and processed in the neuropil of individual cells. This technique can be extended to the entire neuron by impaling and staining a neuron with one microelectrode and then using a second microelectrode to

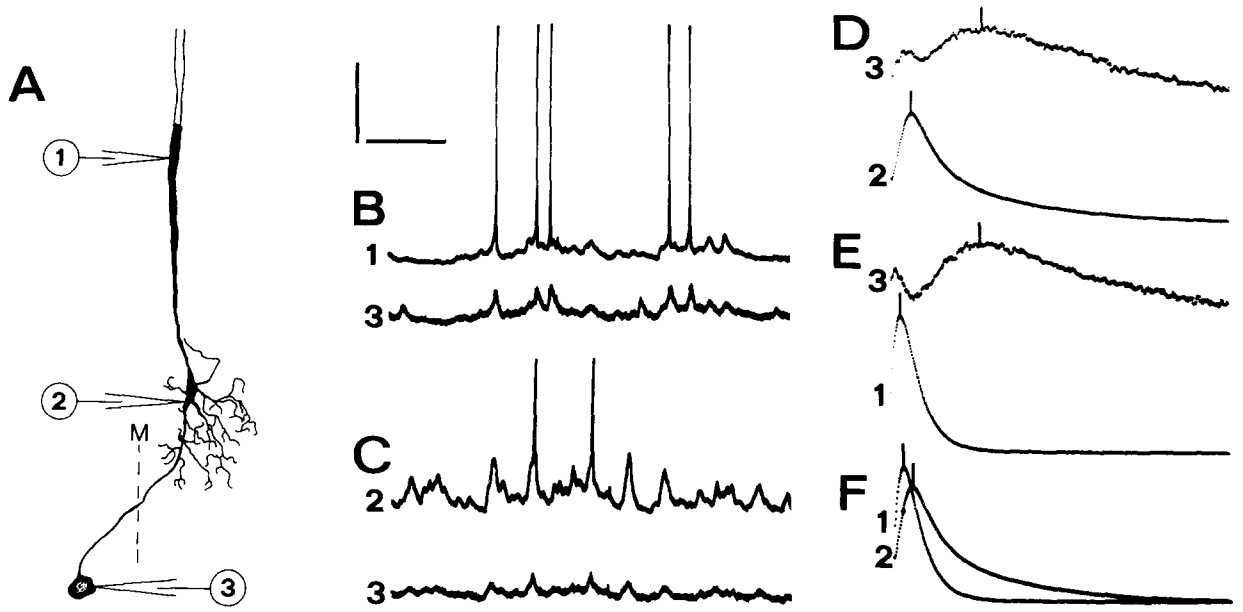

Fig. 7A–F. Intracellular recordings from cell body, neuropil and axon of a crayfish interneuron are sequentially established under visual control. **A** Drawing of the structure of a crayfish sensory interneuron as seen after histological processing. This interneuron, 6B1, was penetrated in its cell body (site '3') and filled with dye from there. Then it was visualized and penetrated with a second microelectrode in the neuropil at site '2'. (The cell body is located on the ventral side of the ganglion, the neuropil site is located approximately 100 µm dorsal to the ventral surface.) After physiological characterization of the interneuron, the second electrode was withdrawn and used to repenetrate the again visualized cell in the initial axon segment at site '1'. **B** Simultaneous intracellular recordings at site '1' and site '3' of ongoing activity in the sensory interneuron. Spikes are severely attenuated in the soma recording ('3') as compared to the axon recording ('1'). **C** Simultaneous intracellular recordings at site '2' and site '3' of ongoing activity in the sensory interneuron. Both spikes and PSPs are severely attenuated in the soma recording ('3') as compared to the neuropil recording ('2'). A comparison of **B** and **C** shows that spikes are attenuated in the neuropil recording '2' as compared to the axon recording '1' and that PSPs are attenuated in the axon recording as compared to the neuropil recording. **D** Signal averaged recordings (10×) of spikes as measured simultaneously in the soma (site '3') and in the neuropil (site '2'). Cursors indicate spike peaks. **E** Signal averaged recordings of spikes as measured simultaneously in the soma (site '3') and in the axon (site '1'). **F** Electronic superposition of the signal averaged soma spikes in **D** and **E** (superposition not shown) allows simultaneous temporal comparison of signal averaged spike forms as recorded sequentially in the initial axon segment (site '1') and in the neuropil (site '2'). Note that crayfish interneurons of this type have single spike initiation sites (Sigvardt et al. 1982). Scale bars: **B** 20 mV, 10 mV, 200 ms; **C** 20 mV, 10 mV, 200 ms; **D, E, F** 3.2 ms

penetrate simultaneously other defined parts of the cell under visual control.

Figure 7 shows an experiment of this kind carried out on an identified sensory interneuron in the crayfish (Sigvardt et al. 1982). The cell was penetrated and filled from the cell body with one microelectrode (Fig. 7A, site '3'). A second microelectrode was then used to penetrate the neuron under visual control at one site in its main neuropil process (Fig. 7A, site '2'). After physiological characterization of the neuron's properties at that site, this second microelectrode was removed from the neuropil and used to repenetrate the cell, again under visual control, at a site in its initial axon segment (Fig. 7A, site '1'). A comparison of the neural activity recorded in the initial axon segment (Fig. 7B, top trace) with that recorded in the dentritic neuropil (Fig. 7C, top trace) shows that spikes are much larger and have a faster time course in the axonal recording than in the neuropil recording. The converse is true for all of the synaptic potentials. These are consistently larger in the dendritic neuropil recording. These data support results which suggest that all synaptic potentials are generated at dendritic sites but that the dendritic membrane of this cell does not produce action potentials (Wine 1975). A comparison of the neural activity recorded in the dendritic neuropil (Fig. 7C, top trace) with that recorded in the cell body (Fig. 7C, bottom trace) shows how much synaptic potentials are attenuated in the soma recording. This is probably due to signal decrement along the electrically inexcitable neurite which connects the soma to the dendritic arbors.

The first microelectrode was used to record the neuron's activity in the cell body throughout this experiment. This reference recording made it possible to confirm that both sequential penetrations

via the second microelectrode were in fact from the identical cell and that this cell's electrical characteristics were not altered by the sequential penetrations. However, the soma recording is useful in another way. The action potentials are severely attenuated in the soma recording. Yet their time of occurrence in the soma can be used as a convenient temporal reference point which allows a direct temporal comparison of the signals recorded in the two sequential penetrations with the second microelectrode. To demonstrate this, signal averaged recordings of spikes measured with both electrodes were carried out, in one case for soma and dendritic recordings (Fig. 7D), in a second case for soma and axonal recordings (Fig. 7E). Electronic superposition of the soma spikes in the two signal averaged traces then allows comparison of the relative time courses of the spike recorded in the axon to that recorded in the dendritic process (Fig. 7F). This shows that peak spike amplitude is recorded in the axon 0.5 ms before it is recorded in the dendritic process, indicating once again that spikes are not initiated in the dendritic neuropil.

The ability to penetrate different parts of a neuron sequentially under visual control is also useful for determining the complete structure of neurons which have long axons. Such neurons will generally not stain along their entire length if dye is injected at a single recording site, due to limited dye migration. However, if dye is injected at one site and the stained parts of the cell are then visualized, a second penetration can be carried out farther along the axon of the cell and dye injected from there. This process can be repeated in an iterative fashion until the entire neuron is filled with dye. Using this technique it has been possible to stain large descending neurons in the locust from an initial recording site in the axonal arbors located in the metathoracic ganglion all the way to the cell's soma and dendritic input sites in the brain; a distance of 1.5 cm (K. Hensler, personal communication; Reichert et al. 1985). The dendritic structure of such cells in the brain of the animal can be visualized in vivo with the same clarity as that of neurons in the segmental ganglia.

Establishing synaptic connectivity between neurons

The problems involved in establishing and maintaining intracellular neuropil penetrations are compounded when simultaneous neuropil recordings from a presynaptic and a postsynaptic cell are required. Yet this is often necessary in order to determine the connectivity between arthropod neurons. During such experiments a major technical difficulty arises whenever one neuron (the presynaptic neuron) has been impaled and one then wishes to find a second neuron postsynaptic to it. The location of the second neuron (the postsynaptic neuron) is usually not known. This necessitates blind probing not only of the ganglion of origin of the presynaptic neuron, but also of other neighboring ganglia. (In principle, the neuropil of the entire nervous system might have to be probed systematically for a postsynaptic cell with the second microelectrode while holding the presynaptic cell with the first microelectrode).

A fast and convenient way to determine the axonal termination site of a presynaptic cell – and thus the probable location of a postsynaptic neuron's neuropil arbors – is to inject dye into the presynaptic cell via the recording microelectrode and then visualize that cell's axonal projections. This allows one to estimate where the sites of axonal termination of the presynaptic cell might be and then probe the neuropil surrounding these sites with a second microelectrode for the postsynaptic cell. Figure 8 shows an example of this type of visually guided connectivity analysis.

A first neuron was penetrated in the mesothoracic ganglion of the locust and partially filled with dye via the recording microelectrode (Fig. 8A, electrode '1'). Laser visualization of the neuron's structure showed it to be an interneuron with soma and dendritic arbors located in the mesothoracic ganglion. The cell's axon bifurcated in this ganglion and projected both rostrally and caudally. The caudally directed axon branch projected to the right half of the metathoracic ganglion. A second microelectrode (Fig. 8A, electrode '2') was then used to probe this part of the metathoracic ganglion for postsynaptic cells. Within several minutes, a neuron was found in this part of the metathoracic ganglion which was apparently postsynaptic to the mesothoracic interneuron. Figure 8A shows the in vivo visualization of both neurons' structure, and Fig. 8B shows the structure of these cells as determined after histological processing. Both show that the metathoracic neuron is a motoneuron. Note also that the axon of the interneuron and the dendritic branches of the motoneuron occupy the same neuropil region. Figure 8C shows that action potentials in the interneuron result in short latency, stable 1:1 EPSPs in the motoneuron. Thus both structure and physiology of these neurons indicate that the interneuron is presynaptically connected to the motoneuron. Both neurons fire rhythmically in phase with wing depressor muscles during flight motor activity (Fig. 8D), indicating that both cells are part of the flight motor of the locust.

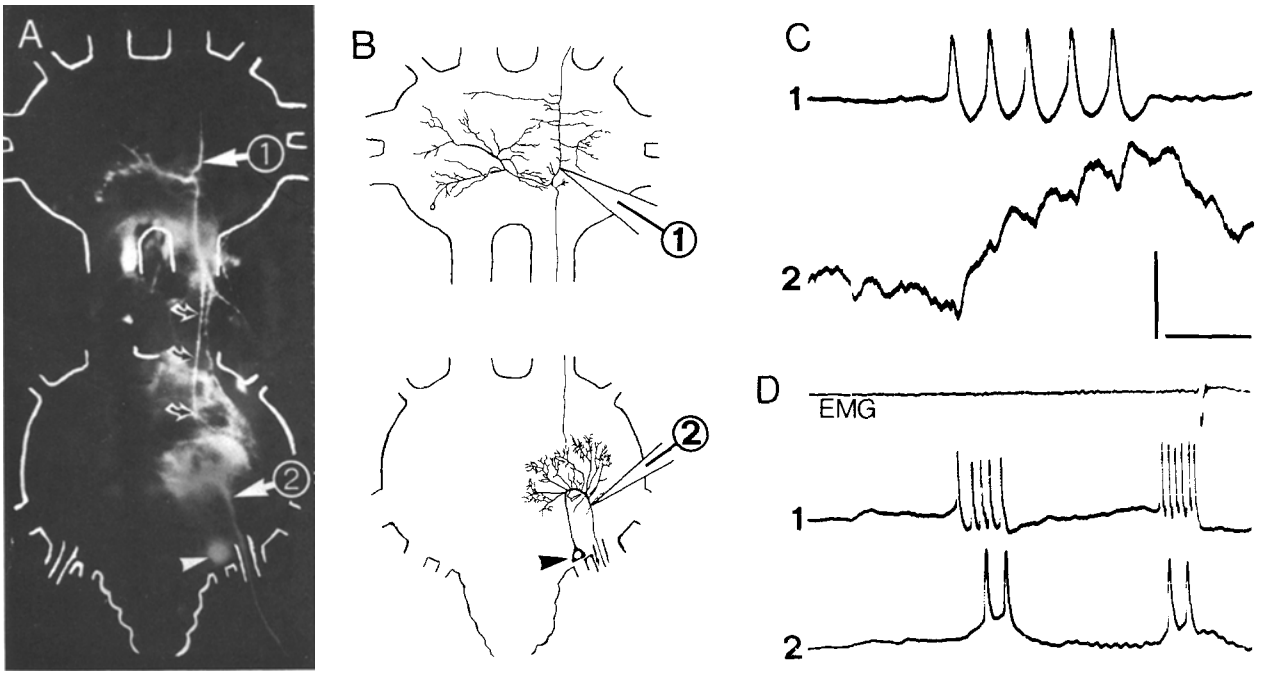

Fig. 8A–D. In vivo visualization of a locust flight interneuron allows rapid localization of a postsynaptic motoneuron. **A** Photomicrograph of both neurons as visualized in vivo. The flight interneuron in the mesothoracic ganglion of the locust was penetrated in the neuropil (arrow indicating site '1') and filled with dye from there. The cell's structure as visualized in vivo revealed a bifurcating axon with one axonal process projecting to the right half of the metathoracic ganglion. The course of this axonal process is indicated by the curved arrows. Subsequently a second microelectrode was used to probe the neuropil in the right half of the metathoracic ganglion for postsynaptic cells. A postsynaptic neuron was penetrated (arrow indicating site '2') and filled with dye. This neuron is a motoneuron with a posteriorly located soma (arrowhead) and an axon which exits the ganglion through nerve 4. **B** Drawing of the structure of both neurons as seen after histological processing. **C** A spontaneous burst of action potentials in the interneuron results in summating 1:1 EPSPs in the motoneuron. **D** During flight motor activity both neurons fire rhythmically in the depressor phase. Top trace, electromyogram of the dorsolongitudinal depressor muscle; middle trace, interneuron recording; bottom trace, motoneuron recording. The muscle did not fire during the first cycle of flight activity. Scale bars: **C** 10 mV, 2 mV, 20 ms; **D** 20 mV, 50 mV, 40 ms

Visualization of dye injection and dye migration

In vivo visualization of Lucifer yellow filled neuronal processes makes it possible to monitor both the extent and the kinetics of intracellular staining. This helps to determine when and if a cell has been adequately filled with dye. It also allows staining and characterization of more than one neuron per ganglion, since confusion of physiology and structure of multiple cells can be ruled out. Moreover, direct observations of the dye injection process reveal the following general features of staining cells with Lucifer yellow:

(i) There is a marked delay before neuropil arbors are filled if dye injection is carried out via the soma. Figure 9A shows a visualization of the staining process for a crayfish sensory interneuron that was filled with dye from its soma using a constant hyperpolarizing current of 4 nA. The outline of the cell body could be detected after less than 30 s. Adequate staining of the interneuron's soma resulted after only 3 min of dye injection. However, staining of the main neuropil arbors required over 30 min and secondary neuropil processes required 60 min for proper staining. We do not know if this delay is due to the soma acting as a sink for dye or if it reflects intrinsic difficulties involved in getting dye through the small diameter neurite connecting soma and neuropil. However, such a long delay before neuropil processes are filled does not occur if dye injection is carried out directly into the neuropil.

(ii) Considerable dye migration can occur after current termination. Figure 9B shows the visualized staining process for another crayfish interneuron that was filled from it's soma by injection of 4 nA of hyperpolarizing current for 10 min. During this time only the cell body and the initial segment of the cell's neurite were dye filled. After 10 min, current injection was terminated and the microelectrode removed from the cell. Nevertheless, in the course of the next hour, dye was seen

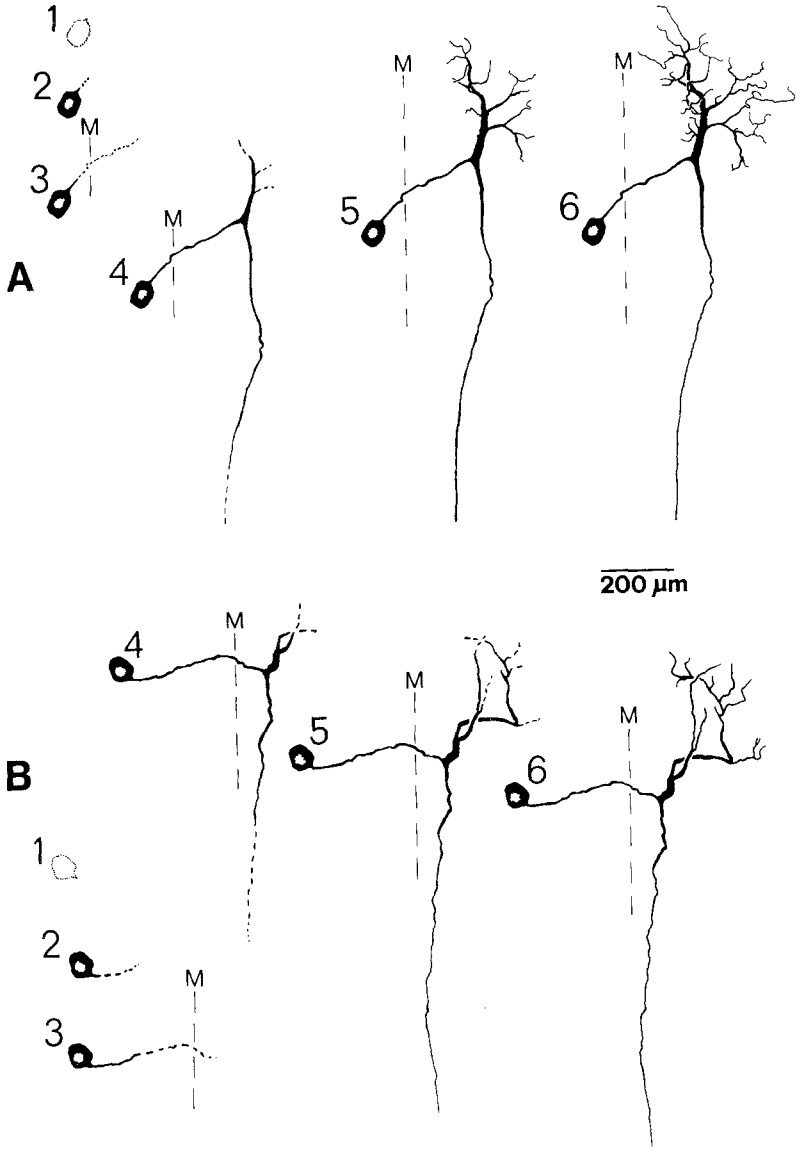

Fig. 9A, B. Visualization of the kinetics of the dye filling process for two crayfish interneurons. **A** A sensory interneuron in the crayfish terminal ganglion was filled with Lucifer yellow dye from it's soma by iontophoretic injection of −4 nA current throughout the course of 60 min. Microelectrode resistance was 50 MΩ. The camera lucida drawings 1–5 indicate the extent of visualized staining at five different times after current injection began (1 = 30 s; 2 = 3 min; 3 = 10 min; 4 = 30 min; 5 = 60 min). After 60 min of dye injection the cell was fixed rapidly and processed for whole mount histology. Drawing 6 shows the extent of staining as seen in a fluorescence compound microscope after histological processing. M indicates the ganglion midline. **B** A second sensory interneuron in the crayfish terminal ganglion was filled with Lucifer yellow dye from it's soma by iontophoretic injection of −4 nA current for 10 min. Microelectrode resistance was 40 MΩ. After the 10 min injection process, current injection was terminated and the microelectrode removed from the neuron's cell body. The drawings 1–5 again indicate the extent of visualized staining at five different times after current injection began (1 = 30 s; 2 = 3 min; 3 = 10 min; 4 = 30 min; 5 = 60 min). (Thus the extent of cell staining at current termination is shown in drawing 3; drawings 4 and 5 show the dispersion of dye in the absence of iontophoretic current.) After 60 min the cell was fixed rapidly and processed for whole mount histology. Drawing 6 shows the extent of staining as seen in a fluorescence compound microscope after histological processing. *M* indicates the ganglion midline

to spread throughout much of the neuron's dendritic arborization. The mechanism of dye dispersion in the neuron after current termination was not investigated. However, a comparison of the dye filling process documented in Fig. 9B with that shown in Fig. 9A suggests that much of the staining in both cases may be due to passive dye dispersion. Moreover, these results indicate that fixation of a neuron immediately following a short dye injection process may actually be detrimental for optimal neuronal staining.

(iii) If dye is injected into extracellular space,

as usually occurs if a penetrated cell is lost in the staining process, Lucifer yellow spreads rapidly in the ganglion and can obscure other filled cells. Subsequent histological processing then reveals 'faint' neuronal staining and a highly fluorescent 'background'.

Discussion

Supravital staining of identified neurons coupled with intracellular recording methods has generated a number of new techniques for cellular neurophysiology. Miller and Selverston's (1978) finding that Lucifer yellow filled cells could be irradiated and killed made it possible to remove identified neurons from neural circuits, to isolate individual neurons from synaptic input and to ablate defined arbors of individual neurons (Miller and Selverston 1979, 1982; Selverston et al. 1984; Jacobs and Miller 1985). Moreover, the finding that Lucifer yellow itself is not obviously toxic when injected into cells (Stewart 1978) allows one to intracellularly label neurons in cell or tissue culture and then observe the morphology of these cells either acutely or over a time course of several days (Kater and Hadley 1982a, b; Gähwiler 1981; Goodman et al. 1982). In this report we show that a modified version of these irradiation paradigms can be useful for obtaining single and multiple intracellular recordings from the neuropil of arthropod neurons in intact adult nervous systems.

We have documented several ways in which laser mediated visualization of arthropod neurons can be used to improve neuropil penetration methodology. However, one important advantage of the technique described here has not been mentioned: namely its simplicity and resulting ease of implementation. Since fiber optics are used, there is no need for a fixed and optically aligned illuminator. There are no space constraints on electrophysiological apparatus and the entire illumination apparatus can be made mobile and so shared among a number of different setups. Focus and intensity of the laser beam are readily adjusted by manually moving the emitting end of the light guide relative to the preparation. Dye-filled cells are illuminated much in the same way as macroscopic objects might be illuminated by a hand held flashlight. No fluorescence compound microscope optics are required, thus the visualization method can be used wherever dissecting microscopes are available. Finally, since the HeCd laser emitts only monochromatic blue light, potentially harmful effects of UV or IR radiation on unstained cells can not occur. (Such effects may occur if broad band irradiation such as that emitted from a Xenon arc lamp is used for fluorescence excitation).

The main disadvantage of the in vivo visualization technique described here is one which is shared with all other fluorescence excitation techniques. This is the fact that it is possible to harm a dye-filled cell by intense or prolonged illumination (Miller and Selverston 1979; Spikes and Livingston 1969). This risk is minimized by reducing illumination time and intensity to the lowest possible level. Additionally, we find it advantageous to inject only relatively small amounts of dye over a time period of many minutes (see Material and methods). In several cases we have repeatedly, albeit briefly, illuminated the same arthropod neuron in experiments which lasted up to three hours with no obvious sign of cell damage. However, the *maximal* intensity provided by the laser illuminator is sufficient to kill neurons reliably if illumination is carried out long enough (3–5 min). Thus, as in all other experiments involving fluorescence based visualization techniques, we find it important to monitor continuously the physiological properties of stained neurons for signs of cell damage whenever they are subjected to an illumination regime.

Acknowledgements. We gratefully acknowledge Drs. J.P. Miller, A.I. Selverston, G. Jacobs and F. Huber for help and advice. We also thank Dr. C.H.F. Rowell for support and for reading the manuscript, Dr. J.M. Camhi for comments on an early draft of the manuscript, Dr. W.W. Stewart for a gift of Lucifer yellow and P. Wehrli for technical support. This work was funded in part by the Schweizerische Nationalfonds (SNF).

References

Gähwiler BH (1981) Labeling of neurons within CNS explants by intracellular injection of Lucifer yellow. J Neurobiol 12:187–191

Goodman CS, Raper JA, Ho RK, Chang S (1982) Pathfinding by neuronal growth cones during grasshopper embryogenesis. Symp Soc Dev Biol 40:275–316

Hedwig B, Pearson KG (1984) Patterns of synaptic input to identified flight motor neurons in the locust. J Comp Physiol A 154:745–760

Hoyle G (ed) (1977) Identified neurons and behavior of arthropods. Plenum Press, New York

Jacobs GA, Miller JP (1985) Functional properties of individual neuronal branches isolated in situ by laser photoinactivation. Science 228:344–348

Kater SB, Hadley RD (1982a) Intracellular staining combined with video fluorescence microscopy for viewing living identified neurons. In: Cytochemical methods in neuroanatomy. Alan Liss Inc, New York, pp 441–459

Kater SB, Hadley RD (1982b) Video monitoring of neuronal plasticity. Trends Neurosci 5:80–82

Kater SB, Nicholson C (eds) (1973) Intracellular staining in neurobiology. Springer, Berlin Heidelberg New York

Krenz WD, Reichert H (1985) Lateralized inhibitory input to an identified nonspiking local interneuron in the crayfish mechanosensory system. J Comp Physiol A 157:499–507

Miller JP, Selverston AI (1979) Rapid killing of single neurons by irradiation of intracellularly injected dye. Science 209:702–704

Miller JP, Selverston AI (1982) Mechanisms underlying pattern generation in the lobster stomatogastric ganglion as determined by selective photoinactivation of identified neurons IV. Network properties of the pyloric system. J Neurophysiol 48:1416–1432

Pitman RM, Tweedle CD, Cohen MJ (1972) Branching of central neurons: Intracellular cobalt injection for light and electron microscopy. Science 176:412–414

Pflüger HJ, Elson R, Binkle U, Schneider H (1986) The central nervous organisation of the motorneurones to a steering muscle in locusts. J Exp Biol 120:403–420

Reichert H, Plummer MR, Wine JJ (1983) Identified nonspiking local interneurons mediate nonrecurrent, lateral inhibition of crayfish mechanosensory interneurons. J Comp Physiol 151:261–276

Reichert H, Rowell CHF (1985) Integration of nonphaselocked exteroceptive information in the control of rhythmic flight in the locust. J Neurophysiol 53:1201–1218

Reichert H, Rowell CHF, Griss C (1985) Course correction circuitry translates feature detection into behavioural action in locusts. Nature 315:142–144

Roberts A, Bush BMH (eds) (1981) Neurones without impulses. Cambridge University Press, Cambridge

Robertson RM, Pearson KG (1982) A preparation for the intracellular analysis of neuronal activity during flight in the locust. J Comp Physiol 146:331–320

Rowell CHF, Pearson KG (1983) Ocellar input to the flight motor system of the locust: structure and function. J Exp Biol 103:265–288

Selverston AI, Miller JP, Wadepuhl M (1983) Cooperative mechanisms for the production of rhythmic movements. In: Roberts A, Roberts B (eds) Neural origin of rhythmic movements. Cambridge University Press, Cambridge, pp 55–88

Sigvardt KA, Hagiwara G, Wine JJ (1982) Mechanosensory integration in the crayfish abdominal nervous system: structural and physiological differences between interneurons with single and multiple spike initiation sites. J Comp Physiol 148:143–157

Spikes JD, Livingston R (1969) The molecular biology of photodynamic action: sensitized photoautoxidation in biological systems. Adv Radiat Biol 3:29

Stewart WW (1978) Functional connections between cells as revealed by dye-coupling with a highly fluorescent naphthalimide tracer. Cell 14:741–759

Strausfeld NJ, Miller TA (eds) (1980) Neuroanatomical techniques. Springer, Berlin Heidelberg New York

Stretton AOW, Kravitz EA (1968) Neuronal geometry: Determination with a technique of intracellular dye injection. Science 162:132–134

Wine JJ (1975) Crayfish neurons with electrogenic cell bodies: correlations with function and dendritic properties. Brain Res 85:92–98